

Effect of aging on the magnetic properties of rapidly quenched Nd-rich Nd-Fe alloys

Dennis Wiafe-Akenteng, Vladimir Menushenkov, Igor Shchetinin, Alexander Savchenko

National University of Science and Technology «MISiS», Leninskiy pr. 4, Moscow, Russia

Abstract. The $\text{Fe}_x\text{Nd}_{100-x}$ ($x = 14, 28$) alloys were successfully prepared by melt-spinning. Hysteretic and thermomagnetic properties of the as-melt-spun alloys and short-aged ribbons were investigated. Both ribbons exhibit a soft magnetic behavior at room temperature but at 5 K, the coercive force (H_{ci}) proliferated to 8.6 kOe and 11.7 kOe, respectively. Thermomagnetic measurements, Zero Field Cooling (ZFC) and Field Cooling (FC), demonstrated that the rise in magnetization of the ribbons at temperatures lower 34 K is associated with ferromagnetism of *fcc* Nd-Fe solid solution clusters. Positive effect of aging on the coercivity of the $\text{Fe}_{14}\text{Nd}_{86}$ and $\text{Fe}_{28}\text{Nd}_{72}$ ribbons was observed. At 300 K, H_{ci} of the ribbons upsurge to 2 - 2.8 kOe after aging at 400 - 450°C for 15 minutes but sharply diminished after aging at temperatures higher than 500°C. It was suggested that the increase in RT coercivity during aging was as a result of the decomposition of the amorphous phase and formation of the hard magnetic Fe-rich clusters. For both ribbons aged at 500°C, the magnetic transition at 340 K was observed to be in relation to the T_C of the $\text{Nd}_2\text{Fe}_{17}$ compound. The appearance of this soft magnetic phase in the microstructure of the aged ribbons was linked with the drastic diminution of the coercivity at that temperature.

1 Introduction

The interest in the study of the Nd-Fe alloys was renewed during the last decades owing to the significant role Nd-rich intergranular phase play in the development of high coercivity of sintered Nd-Fe-B-based magnets. Usually, a high coercivity in the sintered magnets is obtained after post sintering aging to produce the optimal microstructure. The effect of the intergranular Nd-rich phase on coercivity was divided into two contributions. The first is the effect of the thin layers between the $\text{Nd}_2\text{Fe}_{14}\text{B}$ grains which consists of amorphous Nd-Fe phase. These layers act to reduce or remove defects at the $\text{Nd}_2\text{Fe}_{14}\text{B}$ grain surfaces. Secondly, they tend to decouple the $\text{Nd}_2\text{Fe}_{14}\text{B}$ grains with respect to magnetic exchange interactions [1].

The motivation for the study of binary Nd-Fe alloys is the large coercivity of 4.5 kOe of as-cast Nd-rich Nd-Fe alloys without any additional processing step. It is considered that the high coercivity is attributed to the Nd-Fe phase with high magnetocrystalline anisotropy [2, 3] which forms during solidification of Nd-rich alloys. The as-cast alloys are characterized by the metastable eutectic structure consisting of the mixture of Nd grains and the amorphous-like Fe-Nd regions denoted in literature as “ A_1 ” phase. The HRTEM imaging from the Fe-Nd regions reveals that A_1 phase is composed of nanocrystals embedded in an amorphous matrix [4-7]. Unfortunately, the components of A_1 regions cannot be identified because of its very fine size.

The coercivity of as-melt-spun Nd-rich alloys is low at room temperature (RT) but increases with decreasing temperature. The microstructure of as-melt-spun Nd-rich alloys consists of an amorphous-like region composed of nanocrystals of unknown phase embedded in an amorphous matrix [6,7]. It is, therefore, expected that aging may lead to additional decomposition of the amorphous phase and formation of the microstructure similar to the one responsible for the high coercivity in as-cast Nd-rich alloys.

In this work, the effect of aging on the magnetic properties - hysteresis loops, thermomagnetic ZFC-FC dependences of $\text{Fe}_x\text{Nd}_{100-x}$ ($x = 14, 28$) as-melt-spun alloys and polycrystalline Nd - in a temperature range of 5-300 K were investigated.

2 Experimental

Two batches of samples – $\text{Fe}_{14}\text{Nd}_{86}$ and $\text{Fe}_{28}\text{Nd}_{72}$ were prepared from starting materials of high purity elements, iron (99.95%) and neodymium (99.9%). The samples were induction melted and casted under argon atmosphere. The ingots were re-melted and quenched by melt-spinning with a copper-wheel speed of approximately 30 ms^{-1} . The aging of the ribbons was performed in vacuum furnace at temperatures ranging from 300–650°C for 15 minutes. Magnetic measurements at temperatures 5 K and 300 K were performed using a Quantum Design PPMS EverCool-II

* Corresponding author: nanaortchere1@gmail.com

magnetometer in the magnetizing field of 90 kOe. The temperature dependence of magnetization (M) on ZFC and FC for the aged ribbons were measured in an operating field of $H = 0.5$ T over a wide temperature range (5 - 300 K). The specimens were prepared in the form of thin disc from the mixture of the ribbon fragments with epoxy. The error bar of H_{ci} values at repeated measurements was less than 3%.

3. Results and discussion

Hysteresis loops of the Fe_xNd_{100-x} ($x = 14$ and 28) as-melt-spun ribbons measured at 300 K and 5 K are shown in Figure 1. At 300 K, the hysteresis loops of the ribbons $x = 14, 28$ showed a soft magnetic behavior with low magnetization and $H_{ci} - 75$ and 15 Oe respectively. However, both samples displayed a hard magnetic behavior at 5 K with an upsurge in coercivity, 8.6 kOe and 11.7 kOe respectively. Maximum value of magnetization in the field of 90 kOe was recorded at 5 K, 4 times as high as the value measured at 300 K. It should be noted that saturation of the hysteresis loops was not achieved even in magnetic field of 90 kOe.

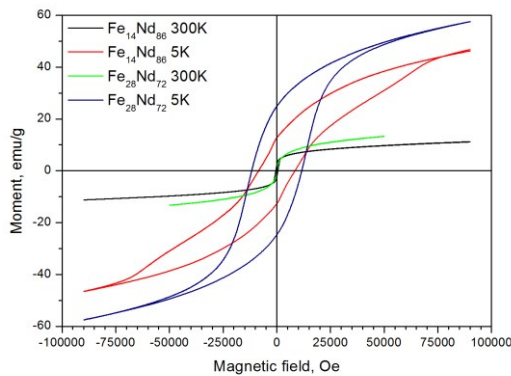


Figure 1. Hysteresis loops of the $Fe_{14}Nd_{86}$ and $Fe_{28}Nd_{72}$ as-melt-spun ribbons measured at 5 K and 300 K

Figure 2a shows a rise in coercivity of $Fe_{14}Nd_{86}$ and $Fe_{28}Nd_{72}$ ribbons when temperature decreases from 300 K to 5 K. The temperature dependence of coercivity show a linear relationship between $H_c^{1/2}$ and $T^{2/3}$ in the temperature range 25 – 200 K (Figure 2b).

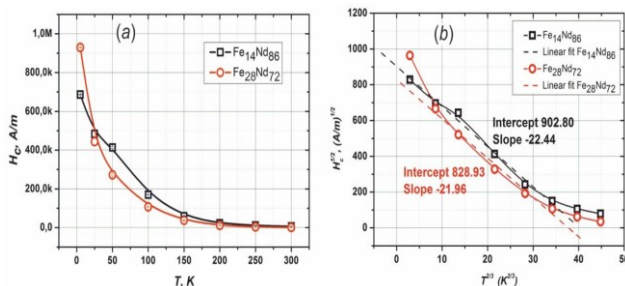


Figure 2. Temperature dependences of $H_c(T)$ (a) and dependences of $H_c^{1/2}(T^{2/3})$ (b) for $Fe_{14}Nd_{86}$ and $Fe_{28}Nd_{72}$ ribbons over the range 5–300 K

These data demonstrate an agreement with strong pinning model of domain walls, proposed by Gaunt [8]. According

to [6,7], the coercivity of the as-melt-spun $Fe_{14}Nd_{86}$ and $Fe_{28}Nd_{72}$ ribbons at lower temperatures is associated with a domain wall pinning on the Nd-rich nanocrystals embedded in an amorphous-like matrix phase which are observed in the ribbons microstructure.

For the interpretation of the temperature dependence of coercivity, temperature dependences of magnetization in the range 5–300 K were made to reveal the possible magnetic transitions. ZFC and FC curves (Figure 3) displays the magnetization behavior of the as-melt-spun $Fe_{14}Nd_{86}$ ribbon and polycrystalline Nd in operating field of $H = 0.5$ kOe over a temperature range 5-300 K. Comparing the ZFC and FC curves for Nd and $Fe_{14}Nd_{86}$ ribbon at temperatures lower than 50 K shows the magnetic transitions at ≈ 9 K, ≈ 17 K and ≈ 34 K in both Nd and ribbon. The observation of these magnetic transitions suggests the presence of several magnetic phases in microstructure of both the crystalline Nd and $Fe_{14}Nd_{86}$ ribbon. According to [9], the first two transitions correspond to antiferromagnetic ordering temperature of the *dhcp* Nd (the onset of ordering on cubic sites). This suggests that the ferromagnetic transition at 34 K is related to the metastable *fcc* allotrope of Nd or Nd-Fe solid solution (Nd-based nanocrystals) [6,7]. Hence, the possible reason for an upsurge in the magnetization at high fields at temperatures lower than 34 K is the presence of *fcc* Nd and Nd-based phases.

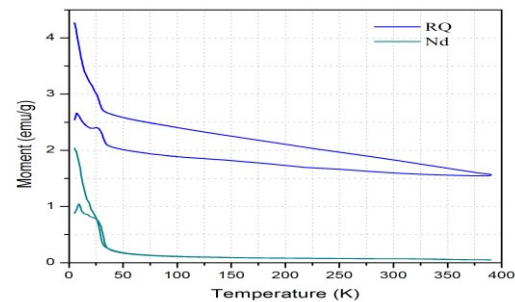


Figure 3. ZFC and FC thermomagnetic curves of the $Fe_{14}Nd_{86}$ ribbon (RQ) and polycrystalline Nd

The paramagnetic susceptibility of the *fcc* Nd and Nd-Fe solid solution resulted in unsaturated magnetization curves for the $Fe_{14}Nd_{86}$ ribbon at temperatures above 34 K. But the fact that saturation of the hysteresis loops is not achieved at 5 K shows the presence of high magnetocrystalline anisotropy of Nd which connotes magnetic moments remain noncollinear down to 5 K. For this reason, the random-anisotropy model [10] of the Fe-contained clusters may be used to explain the magnetic properties of as-melt-spun ribbons. In the zero field, the magnetization moments of the Nd-Fe clusters are directed along the easy axes which have random orientation. An increasing magnetic field overcomes the anisotropy energy and aligns the magnetization moments of the clusters towards the field direction.

It was observed that a short aging of the $Fe_{14}Nd_{86}$ and $Fe_{28}Nd_{72}$ ribbons at temperatures lower than the eutectic temperature in Fe-Nd system (685°C) increased the coercivity. It might be as a result of transforming their microstructure which was composed of Nd-based nanocrystals and residual amorphous phase. It could also

be caused by decomposition of the amorphous phase and precipitation of the Fe-rich clusters with high magnetocrystalline anisotropy which increased the coercivity. On the other hand, the precipitation of the soft magnetic $\text{Fe}_2\text{Nd}_{17}$ clusters resulted in lessening the coercivity. Secondly, the increase of the size of Nd-rich nanocrystals during aging may have resulted in the nanocrystals losing the role as the domain walls pinning centers.

The hysteresis loops of the $\text{Fe}_{14}\text{Nd}_{86}$ and $\text{Fe}_{28}\text{Nd}_{72}$ ribbons measured at 300 K and 5 K after aging at 300 – 600°C for 15 minutes are shown in Figures 4 and 5 respectively. The temperature dependences of coercivity for the $\text{Fe}_{14}\text{Nd}_{86}$ and $\text{Fe}_{28}\text{Nd}_{72}$ ribbons over the aging temperature range 300–600°C are shown in Figure 6. Maximum values of coercivity, 3.1 kOe and 2.6 kOe, were received after aging at 400 - 450°C for the ribbons $x = 14, 28$ respectively measured at 300 K. These values of coercivity is only slightly less than the coercivity of as-cast Nd-rich Fe-Nd alloys, $H_{ci} = 4\text{-}4.5$ kOe [2,3]. Aging at temperatures higher than 450°C recorded a reduction in coercivity for the $\text{Fe}_{14}\text{Nd}_{86}$ and $\text{Fe}_{28}\text{Nd}_{72}$ ribbons.

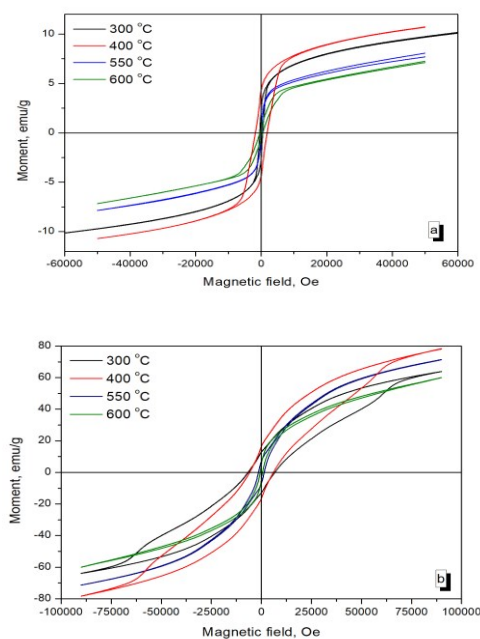


Figure 4. Hysteresis loops of the $\text{Fe}_{14}\text{Nd}_{86}$ ribbons after aging at 300–600°C for 15 min measured at 5 K (a) and 300 K (b)

As seen in Figure 6a, at 5 K, the coercivity of as-melt-spun $\text{Fe}_{14}\text{Nd}_{86}$ and $\text{Fe}_{28}\text{Nd}_{72}$ ribbons (8.6 kOe and 11.7 kOe, respectively), slightly reduced after aging in the temperature range of 300 – 450°C and decreased drastically after aging at 500°C and higher temperatures. At 300 K, the coercivity of as-melt-spun ribbons $\text{Fe}_{14}\text{Nd}_{86}$ and $\text{Fe}_{28}\text{Nd}_{72}$ (75 and 15 Oe, respectively) rose to 2 - 2.8 kOe after aging at 400 - 450°C. A sharp drop was observed after aging at temperatures higher than 500°C.

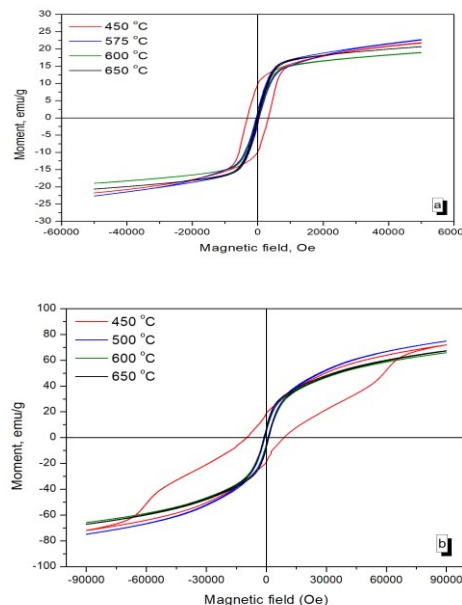


Figure 5. Hysteresis loops of the $\text{Fe}_{28}\text{Nd}_{72}$ ribbons after aging at 300–600 C for 15 min measured at 5 K (a) and 300 K (b)

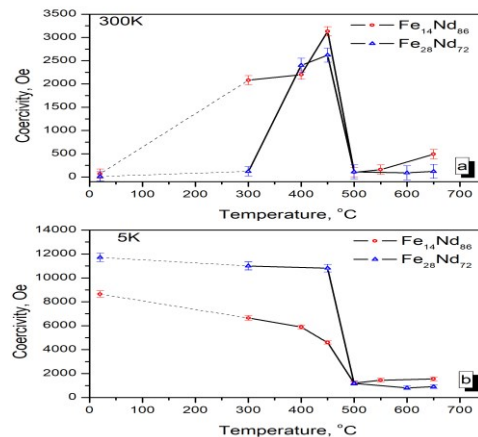


Figure 6. Dependences of H_c versus the aging temperature for the ribbon $\text{Fe}_{14}\text{Nd}_{86}$ (a) and $\text{Fe}_{28}\text{Nd}_{72}$ (b) measured at 5 K and 300 K after aging at 300 – 650 C for 15 min

For the interpretation of this data, it was suggested that the main reason for an increase in RT coercivity after short aging at 400 - 450°C is decomposition of the amorphous phase and formation of the Fe-rich clusters of the hard magnetic phase like that in as-cast Nd-Fe alloy. The low level of coercivity of the aged ribbons at 300 K (1.8 - 2 kOe) in comparison with H_{ci} of the as-cast alloy (4.5 kOe) can be explained as due to the non-optimal composition or size of the Fe-rich clusters and a coarsening of the Nd-rich nanocrystals during aging hence decreasing the domain wall pinning.

Figure 7 shows the ZFC and FC thermomagnetic curves of the ribbons $\text{Fe}_{14}\text{Nd}_{86}$ (a) and $\text{Fe}_{28}\text{Nd}_{72}$ (b) after aging at 300 – 650 C for 15 minutes. The comparison of the ZFC and FC curves of $\text{Fe}_{14}\text{Nd}_{86}$ and $\text{Fe}_{28}\text{Nd}_{72}$ ribbons after melt spinning and after aging in Figures 3 and 7

shows that aging has no effect on the temperature of the bends on the $M(T)$ curves at temperatures lower than 50 K. Hence, the composition of Nd or Nd-based solid solution in these ribbons remains unchanged.

As demonstrated in Figure 7, the temperature dependences of magnetization (FC) for the $\text{Fe}_{14}\text{Nd}_{86}$ and $\text{Fe}_{28}\text{Nd}_{72}$ ribbons aged at temperatures 300 - 450°C shows that magnetic transition (T_C) takes place at temperatures higher than 500 K. But for both ribbons aged at 500°C, the magnetic transition was observed at 330-340 K which is close to the T_C of the $\text{Nd}_2\text{Fe}_{17}$ compound (335 K). The appearance of this soft magnetic phase in the microstructure of the aged ribbons resulted in drastic decrease in the coercivity.

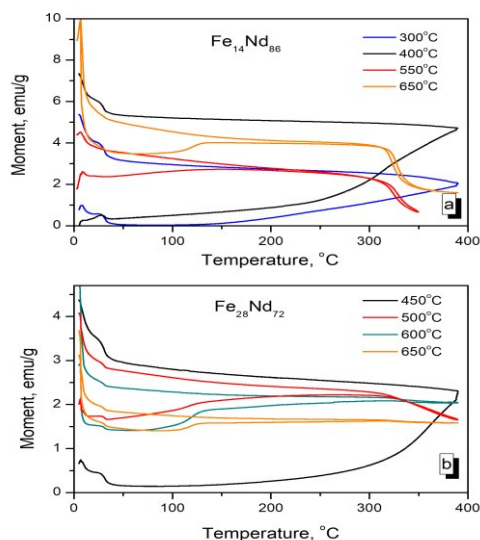


Figure 7. Zero-field cooling (ZFC) and field cooling (FC) thermomagnetic curves of the ribbon $\text{Fe}_{14}\text{Nd}_{86}$ (a) and $\text{Fe}_{28}\text{Nd}_{72}$ (b) after aging at 450 – 650 C for 15 min

Based on the obtained data, it can be discussed that the possible mechanism of the intergranular phase has an influence on the H_{ci} of sintered magnets during post-sintering aging. Usually, in sintered magnets the Nd-rich intergranular phase is an amorphous region similar to the amorphous-like phase in as-melt-spun Nd-rich ribbons. It may be assumed that the post-sintering aging of the ribbons led to the decomposition of the intergranular amorphous phase and appearance of the Fe-Nd clusters, similar to the clusters in as-melt-spun ribbons that resulted in a rise in the H_{ci} of aged magnets.

Conclusion

Hysteretic and thermomagnetic properties of the $\text{Fe}_{14}\text{Nd}_{86}$ and $\text{Fe}_{28}\text{Nd}_{72}$ as-melt-spun alloys and short aged ribbons were investigated. The present study showed that as-melt-spun ribbons exhibit a soft magnetic behavior at room temperature but with decreasing temperature from 300 to 5 K, H_{ci} proliferated up to 8.6 kOe and 11.7 kOe, respectively. The increase in H_{ci} can be associated with a domain wall pinning on the Nd-rich

nanocrystals embedded in an amorphous-like matrix which were observed in the microstructure of the ribbons.

Thermomagnetic measurements (ZFC and FC) for the as-melt-spun $\text{Fe}_{14}\text{Nd}_{86}$ and $\text{Fe}_{28}\text{Nd}_{72}$ ribbons show magnetic transitions at 9, 17 and ≈ 34 K. The first two transitions, 9 and 17K, originated from *dhcp* Nd and the third transition is associated with ferromagnetism of *fcc* Nd-Fe solid solution which resulted in an increase of the magnetization of the ribbons at temperature lower than 34 K.

The positive effect of aging on the H_{ci} of the as-melt-spun $\text{Fe}_{14}\text{Nd}_{86}$ and $\text{Fe}_{28}\text{Nd}_{72}$ ribbons was observed. At 300 K, the H_{ci} of the as-melt-spun ribbons (75 and 15 Oe, respectively), escalated to 2 - 2.8 kOe after aging at 400 - 450°C but sharply declined after aging at temperatures higher than 500°C. It was suggested that the main reason for the rise in RT H_{ci} during aging is the decomposition of the amorphous phase and formation of the hard magnetic Fe-rich clusters. For both ribbons aged at 500°C, magnetic transition was observed at 340 K, closer to the T_C of the $\text{Nd}_2\text{Fe}_{17}$ compound ($T_C = 335$ K). The appearance of this soft magnetic phase in the microstructure of the aged ribbons resulted in H_{ci} reducing drastically.

Further studies must be mainly directed to structural analysis of the aged samples to help clarify the effect of aging on its magnetic properties.

Acknowledgement. This work was supported by the Ministry of Education and Science of the Russian Federation (agreement no. 14.587.21.0028, a unique no. RFMEFI58716X0028).

References

- [1] T.G. Woodcock, Y. Zhang, G. Hrkac, G. Ciuta, N.M. Dempsey, T. Schrefl, O. Gutfleisch, D. Givord. *Scripta Materialia* 67 (2012) 536.
- [2] Drozzina V, Janus R. *Nature*, 1935, 135, 36.
- [3] J.J. Croat, *Appl. Phys. Lett.*, 1981, 39, 357.
- [4] V. P. Menushenkov, A. S. Lileev, M. A. Oreshkin, S. A. Zhuravlev, *J. Magn. Magn. Mater.*, 1999, 203, 149.
- [5] Kumar, J. Eckert, S. Roth, W. Loser, L. Schultz, S. Ram. *Acta Materialia*, 51 (2003) 229.
- [6] Menushenkov, V. P., Shchetinin, I. V., Gorshenkov, M. V., Savchenko, A. G., & Ketov, S. V. (2016). *IEEE Magnetics Letters*, 7, 1-4.
- [7] V.P. Menushenkov, I.V. Shchetinin, M.V. Gorshenkov, A.G. Savchenko, S.V. Ketov, Proc. of the 24-th Int. Workshop on Rare-Earth and Future Permanent Magnets and their Applications (REPM 2016), 2016, Darmstadt, Germany.
- [8] P. Gaunt. *Philos. Mag. B*, 1983, 48, 261.
- [9] E. Bucher, C. W. Chu, J. P. Maita, K. Andres, A. S. Cooper, E. Buehler, and K. Nassau, *Phys. Rev. Lett.*, 1969, 22, 1260.
- [10] R. Ribas, B. Dieny, B. Barbara, A. Labrata, *J. Phys. Condens. Matter*, 1995, 7, 3301.